As per UGC guidelines an electronic bar code is provided to secure your paper

International Journal for Modern Trends in Science and Technology
Volume 10, Issue 11, pages 34-47.
ISSN: 2455-3778 online
Available online at: http://www.ijmtst.com/vol10issue11.html
DOI: https://doi.org/10.46501/IJMTST1011005

Integrated Standalone Wind and Solar to Electric Vehicle Technology with Battery Microgrids in DC Fast Charging Architecture for Sustainable Mobility Initiative

Dr. J. Srinu Naik | P. Bhanu Prakash | M.V.S. Durga Prasad | B. Karthik Kumar Reddy | P. Sai Narasimha Reddy T

Department of Electrical and Electronics Engineering, Chadalawada Ramanamma Engineering College, Andhra Pradesh, India.

To Cite this Article
Dr. J. Srinu Naik, P. Bhanu Prakash, M.V.S. Durga Prasad, B. Karthik Kumar Reddy, P. Sai Narasimha Reddy T, Integrated Standalone Wind and Solar to Electric Vehicle Technology with Battery Microgrids in DC Fast Charging Architecture for Sustainable Mobility Initiative, International Journal for Modern Trends in Science and Technology, 2024, 10(11), pages. 34-47. https://doi.org/10.46501/IJMTST1011005

Article Info
Received: 29 October 2024; Accepted: 22 November 2024.; Published: 25 November 2024.

Copyright © Dr. J. Srinu Naik et al; This is an open access article distributed under the Creative Commons Attribution License, which permits unrestricted use, distribution, and reproduction in any medium, provided the original work is properly cited.

ABSTRACT

This paper presents a novel approach to electric vehicle (EV) charging infrastructure, integrating solar and wind power with a battery charging station. The system aims to reduce environmental impact and enhance energy resilience while meeting increasing EV charging demands. The Perturb and Observe Maximum Power Point Tracking (MPPT) algorithm optimizes the charging process, extracting maximum power from renewable energy sources. Simulation results show the integrated system consistently achieves high levels of energy harvest from solar and wind sources, ensuring efficient utilization of renewable energy. The system adapts to changing environmental conditions, dynamically adjusting charging parameters to maximize energy capture. Surplus energy stored in station batteries serves as backup power, ensuring uninterrupted EV charging during climate change-induced disruptions. The simulation-based analysis validates the feasibility and efficacy of the proposed integrated approach, underscoring the importance of renewable energy integration and efficient charging algorithms in advancing environmentally friendly transportation solutions.

KEYWORDS: Electric vehicle (EV), solar power, Wind power, Battery technology, Maximum Power Point Tracking (MPPT) algorithm

1.INTRODUCTION

The world's electrical energy generation is a major contributor to many forms of pollution. The burning of fossil fuels in thermal power plants (coal, oil) causes emissions that are connected to air pollution. Nuclear power facilities, whose construction ramped up in the wake of the oil crisis, have so far failed to degrade air quality. But they also generate radioactive waste, which poses serious challenges in handling, processing, and transporting the material. In today's energy production market, renewable energies such as hydropower, wind, solar, biomass, etc., play a significant role due to the openness of the market and the concern of relying on a single, potentially dangerous energy source [1, 2]. Phasing issues between generated and consumed energy occur because consumer demand for energy is often not uniformly distributed throughout time. Production and consumption must be balanced for the grid to remain stable [3]. The use of electrical energy storage systems, which are often associated with renewable energy sources, will encourage their involvement in various services, which in turn will condition the rise in the penetration rate of renewable energies [4]. Consequently, the power grid's ability to store these energy is crucial to their integration. The grid operator may achieve a real-time balance between production and consumption using this technological approach. Additionally, renewable resources can be used to their full potential by preventing load shedding when output exceeds demand. As an added bonus, decentralised storage, when coupled with local renewable production, might allow for the islanding of the region served by this resource, making the electrical network more resilient. Power given during peak hours is much more valuable when it comes from an energy storage system (ESS) that is strategically situated because it improves control over frequency and voltage and mitigates the effects of power fluctuation by boosting the value of the current supplied [5, 6]. New study is focusing on how to combine renewable energy sources with energy storage in a freestanding micro grid. Combining various renewable energies, such as tidal, wind, and PV, is ideal since it increases the system's maximum capacity for energy storage. Supercapacitors and batteries work together to form ESS, which allows for a rapid system reaction to offset transients and prolongs the life of the batteries [7]. In contrast to supercapacitors, the AC grid is used when all energy sources and BSSs are linked, as loads are required [8]. The microgrids may be either direct current (DC) or alternating current (AC), or they might be hybrids of the two. With DC microgrids, there are fewer control parameters, easier integration, and a simpler structure compared to AC microgrids. Control design becomes more difficult with AC type because additional information is required, such as frequency and reactive power synchronisation. There are a number of modes that a DC micro grid may operate in, including AC microgrid, standalone, and integrated [9], [10]. Thanks to cutting-edge advancements in power electronics, the autonomous DC microgrid is able to thrive. Nevertheless, an additional energy management unit is required for the renewable energy sources' stochastic character to ensure continuous power transfer to the loads and smooth operation. Given the significant differences in the dynamics of AC and DC microgrids, control techniques developed for AC microgrids cannot be used to DC microgrids, despite the abundance of literature on the topic. A DC microgrid's typical layout really involves a DC-link for both power consumption and supply, as well as a parallel connection between the load converters and the energy sources. As a result, a DC microgrid cannot function efficiently and reliably without controlling the DC-link voltage [11], [12]. The DC-link voltage problems have prompted the publication of many control techniques. There has been a lot of progress in the field of hybrid micro grid topology, which incorporates energy resource planning and control, as discussed in [13]. One method for controlling the DC voltage is suggested in [14] using a fuzzy controller in conjunction with voltage control. In [15], the authors go into the topic of fuzzy logic control strategies that use fewer rules. Using a dual proportional-integral controller is done in [16]. Nevertheless, the control procedures described earlier are linear and have the ability to regulate the DC-link inside a little functioning period. Notwithstanding this limitation, research on nonlinear controls has been conducted in academic journals. The method for an adaptive droop controller is suggested in [17]. In a microgrid, a number of energy storage systems are examined in relation to energy management-based optimum control in [18]. Developed in [19] is a comprehensive method for H1 control. An

approach with a robust sliding mode is suggested in [20]. An adaptive backstepping control mechanism is established in [21]. A technique based on Lyapunov is described in [22], and feedback linearization control is addressed in [23]. In terms of controller design, [24] explores a hybrid that combines backstepping and sliding mode. Optimal energy management has provided a multiple integrated energy storage system, although earlier suggested nonlinear controls have flaws in stability for the H1 approach and chattering problems with the sliding mode. Additionally, droop control strategies have limited performance. The fixed gains that these controls rely on are also very vulnerable to shocks from the outside world and parameter uncertainty. This whole thing culminates in the energy management component. Simultaneously, this study proposes a novel PI controller to solve the issues with traditional integer controllers in hybrid energy management. Simplicity and performance are both met by the suggested PI controller. The two primary goals of this study are to first, use the suggested PI controller to maximise power extraction from wind and PV by managing the source-side converters (SSCs), and second, to solve these issues. The optimisation of electric vehicle (EV) power management performance inside a microgrid is the second objective. A Perturb and Observe (P&O) Maximum Power Point Tracking (MPPT) algorithm is used to regulate renewable energy sources and controls the DC-link voltage to meet established references. There are chances for environmentally friendly EV charging solutions with the incorporation of microgrids that use renewable energy sources, such as wind and solar power. But to successfully manage the charging process, advanced management mechanisms are needed, as renewable energy supply is intermittent. By monitoring the highest possible power production from renewable sources, the P&O MPPT algorithm guarantees maximum efficiency and power harvesting. Important for the efficiency and stability of the microgrid, the energy management unit (EMU) keeps an eye on the DC-link voltage. Electric vehicles are guaranteed a steady supply of electricity by use of the EMU, which regulates the voltage to previously established setpoints. The EMU uses real-time data to coordinate charging schedules, giving preference to renewable energy use for EV charging, which in turn reduces reliance on traditional grid sources and promotes sustainability. Additionally, batteries serve as a supplementary power source, providing backup power during periods of low renewable energy generation or high demand.

II. SYSTEM CONFIGURATION

The proposed integrated EV charging infrastructure uses solar panels to generate direct current (DC) electricity, which is converted to a compatible form for charging EVs using a solar DC-DC converter. Wind turbines generate alternating current (AC) electricity, which requires conversion to DC for integration into the charging network. A wind AC to DC rectifier converts the AC output from the turbines into a stable DC output. A wind DC-DC converter adjusts the voltage and current levels of the wind-generated DC power to optimize its compatibility with the charging infrastructure. A bidirectional DC-DC converter is incorporated for battery charging and electric vehicle integration, enabling the charging of the battery energy storage system (BESS) when surplus energy is available from renewable sources. This ensures efficient utilization of renewable energy sources while meeting EV charging demands, contributing to a sustainable and resilient mobility ecosystem as shown in figure 1.

III. MICRO GRID SYSTEM MODEL AND DESIGN

A. Solar Photovoltaic Panel Modeling and Performance Parameters

a. Solar Photovoltaic Panel Modeling

The layout of basic idea for a hybrid renewable energy system using the PV model. Here, we zero in on the PV cell type seen in Fig. 2 that has a single diode. For a depiction of the equivalent circuit of a solar PV panel using a single diode, refer to Figure 2.

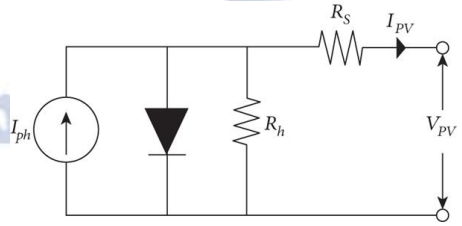

Figure 2 Equivalent circuit of PV panel.

As shown in equation (1), a PV panel's output current may be calculated.

$$I_{PV} = N_P I_{Ph} - N_P I_o \left(exp \left[\frac{q(V_{PV}/N_S + I_{PV} R_S/N_P)}{nkT} \right] - 1 \right) - \frac{V_{PV} + I_{PV} R_S}{R_h} \quad (1)$$

This is where the following symbols are defined: V_{PV}, which stands for the voltage generated by the PV panel; I_o, for output current; I_{Ph}, for input current; and I_{PV}, for input current from the light source. R_h and R_s are the shunt and series resistances, respectively. N_P stands for the total number of cells linked in parallel, whereas N_s represents the number of cells linked in serial. The ideal diode has a value of 1, and the variables K, T, q, and n stand for Boltzmann's constant, the temperature of the PV panel, the charge on an electron, and the ideality of the diode, respectively ($1 \cdot 602 \times 10^{-19} C$, $1.38 \times 10^{-23} J / k$),. The temperature of the PV panel influences both Io and (I_{Ph}), while irradiance (G) only influences the light generated current (I_{Ph}). Eq. (2) shows how temperature affects the reverse saturation current (I_o), and Eq. (3) shows how temperature and irradiance affect the light-generated current [25]. For further information on how to simulate PV arrays, see [25].

$$I_0 = I_{0,n}\left(\frac{T_n}{T}\right)^3 exp\left(\frac{qE_{go}}{nk}\left(\frac{1}{T_n}-\frac{1}{T}\right)\right) \quad (2)$$

$$I_{Ph} = \left(I_{Ph,n} + k_1(T - T_n)\right)\frac{G}{G_n} \quad (3)$$

The following variables are defined: T_n = 25°C, Gn = 1000 watts/sq. m., I_o,n = saturation current, I_{Ph},n = light current, E_{go} = energy across the bandgap of the solar cell, and k_1 = reference temperature coefficient for a short circuit.

.

b. Characteristics of Solar PV Panel

The nonlinearity between Ipv and Vpv is fairly considerable, the diode in the same circuit considerably affects the I-V characteristics of the solar cell, and the connection between the two is not linear, as can be seen from equations (1)–(3). With one parameter kept at its STH value and the other changed, we simulate the I-V and P-V characteristics at two irradiance levels and temperatures to examine the effect of these two variables. For irradiances of 500 W/m^2 and 1000 W/m^2 maintained at 25°C, Figure 3 shows the simulated current-voltage and current-polarity characteristics. Although short-circuit current is linear with respect to irradiance, open-circuit voltage is not. The highest amount of power that may be produced is therefore directly related to the amount of radiation that is applied.

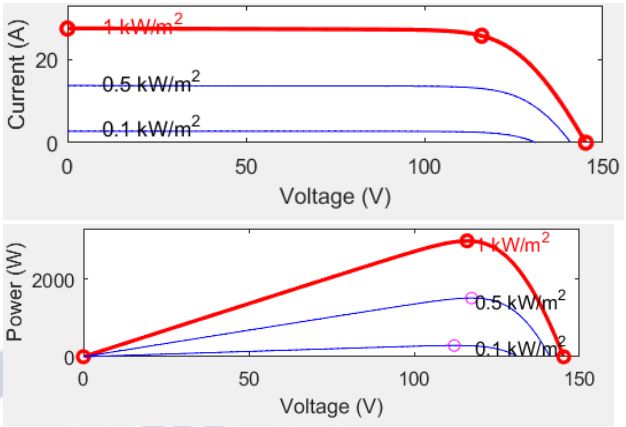

Figure 3 I-V and P-V characteristics of a PV panel.

Spectral lines Shaded areas, caused by objects such as clouds, trees, birds, and buildings, significantly reduce the efficiency of solar panels [25]. The need of efficient power management systems that can adapt to partial shade conditions is shown by this. Therefore, further steps, such as the usage of bypass diodes, may be required to mitigate the effects of partial shadow. The idea for the suggested PVE came from wanting to simulate how a PV panel would respond to two simultaneous irradiation levels. To investigate the characteristics of a partially shaded PV panel, we maintain a constant temperature of 25°C and subject the exposed cells to 1000 W/m^2, while the shaded cells get 300 W/m^2.

Table .1 Parameter Specifications of BP Solar 1Soltech 1STH-215-P PV Module

Description	Ratings
Maximum power (PMP)	213.15 W
Maximum current (IMP)	7.35 A
Maximum voltage (VMP)	29 V
Short circuit current (ISC)	7.84 A
Temperature (T)	$25^0 C$
Open circuit voltage (Voc)	36.3 V
Parallel strings	3.5
Series-connected modules per string	4
Solar irradiation (G)	1000W/m2

c. Solar energy conversion system (SECS)

A maximum power point tracking (MPPT) controller, a DC-DC boost converter, and solar photovoltaic panels comprise the SECS. The charge level of the battery storage system determines whether the MPPT is in active or standby mode. The MPPT controller continuously checks the voltage and current output of a

solar PV panel. In order to transfer solar energy to the batteries as effectively as possible, it optimises the operating point of the DC-DC boost converter. The battery will be charged effectively and solar energy will be utilised to its maximum capacity.

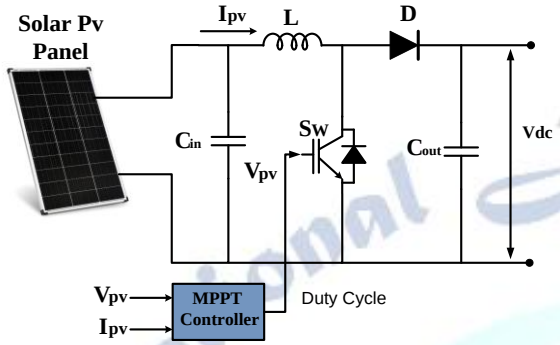

Figure 4 boost converter configuration of solar system with P&O MPPT controller

Perturbation and observation (P&O): This method employs real-time optimisation of the voltage. While there are more advanced and effective variations of this strategy, we've included a simple P&O MPPT algorithm below for demonstration purposes. The maximum power point tracking (MPPT) algorithm is a feature of photovoltaic (PV) inverters that ensures the system operates at or near the PV panel's peak power point even when temperature, load, and solar irradiation change. Solar converter engineers improve PV system output using P&O MPPT algorithms. The algorithms' management of the voltage ensures that the system remains at its "maximum power point" (peak voltage) along the power voltage curve. Numerous MPPT algorithms are included into controller designs for PV systems.

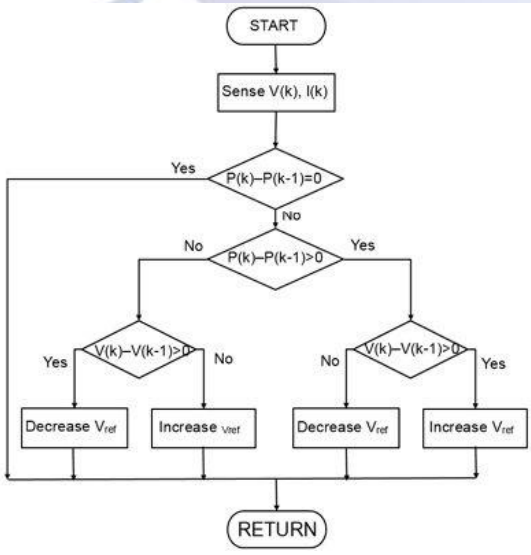

Figure 5 The perturb and observe algorithm flow chart for a solar DC-DC converter.

Algorithms account for environmental factors like temperature and fluctuating irradiance (sunlight) to ensure that the PV system maintains its maximum power output.

B. Small-Scale Wind-Turbine System

The Indonesian government has been investigating wind power as a possible means of reducing the country's impact on global warming. Wind turbines may be gaining popularity in Indonesia due, in part, to the country's pleasant climate. Indonesia is prone to tropical winds, which may reach speeds of 3–15 m/s [27]. Small wind turbines will be used by the majority of people to do this [28]. An apparatus that spins in response to the kinetic energy of the wind is called a turbine. The sum of the kinetic energy is a function of both the wind speed and air density [26]. You may use this formula to show the power that the wind turbine system produces:

$$P = 0.5C_P\rho AV^3 \quad (4)$$

Equation (4) shows that the mechanical energy output of the wind turbine is determined by the coefficient of kinetic power (Cp). The ability of the wind turbine to transform kinetic energy is affected by many factors. The blade tip speed ratio is one of the factors that affect the quantity of power produced by wind turbines. The angle between the turbine's pitch blades and the wind velocity produces this ratio. The speed ratio may be seen as the ratio of the change in time between

$$\lambda = r\omega / v \quad (5)$$

The electrical output of a wind turbine system may be calculated by inserting Eq. (5) into Eq. (4).

$$P = 0.5C_P\lambda\rho A(r / \lambda)^3(\omega)^3 \quad (6)$$

The additional torque may be determined by applying Equation (6):

$$P = 0.5C_P\rho A(V / \lambda) \quad (7)$$

Equation (7) shows that there is a speed range in which the power coefficient may be optimised. Wind turbines may generate the most power when the ratio of wind speed to blade rotation speed is one to one. Figure

6 shows the variation in output power for various wind speeds at a pitch angle of zero degrees. Mechanical power is directly related to rotation speed, since the winds range from 4 to 12 metres per second. In this case, producing 3 MW of mechanical power at 1 p.u. requires a wind speed of 12 m/s.

a. Controlling Maximum Power Point Tracking (MPPT) with an Enhanced Perturb and Observe (P&O) Algorithm

i. Maximum Power Point Tracking for Domestic Wind Turbines

A wind turbine, as shown in Figure 7, typically consists of the following parts: the turbine, a boost converter (used to convert three-phase AC power to DC), a generator-side converter, and a permanent magnet synchronous generator (PMSG). In order to get the most out of the rectifier in the wind generator, the MPPT controller is constantly modifying the operating point. No matter the direction or speed of the wind, this controller will keep the wind turbine system running at full efficiency. Additionally, the MPPT Controller prevents the system from being overworked or overheated, which increases its reliability and longevity [29]. A wind turbine is one device that can collect and use wind energy. An approach to finding the wind turbine's power output is to use Equation (4), which considers the air type's mass density (ϱ), the cross-sectional area (A), and the third power of the wind velocity (V^3).

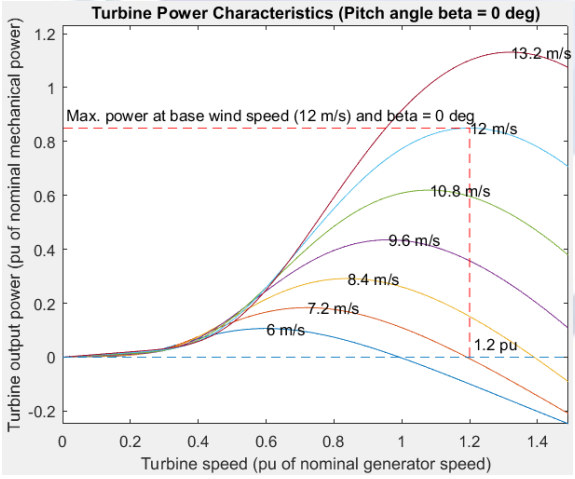

Figure .6 Wind turbine characteristics with pitch angle of 0^0.

A generator may be powered by the wind via the rotation of a shaft, which spins a turbine. Depending on the tip speed ratio, a wind turbines power coefficient (CP) a property can be anywhere from 25% to 45%, indicating the maximum power production. Generators are responsible for converting the torque (T) and rotor speed (ὐ) of a turbine into voltage (V) and current (I), respectively, in order to produce electricity. It is possible to produce three-phase alternating current with this power plant. Since the rotor of a permanent magnet synchronous generator (PMSG) acts as the excitation source, no additional excitation apparatus is required [26]. The system becomes much simpler when voltage control is not needed. It is common practice to use PMSGs in medium and low capacity wind turbines in order to convert wind energy into electricity. Although the wind speeds in Indonesia are often not particularly powerful, it might nevertheless be beneficial for small-scale power facilities there. Despite the PMSG's cheap price, simplicity, durability, and less complex clutch grid, the main negative [30] is the necessity for smaller power factor and efficiency compensators. With this fresh method, we can harness the wind's power for real-world use. The output power of wind energy systems is sensitive to changes in wind speed [31, 32]. Peak power generation is guaranteed via maximum power point tracking (MPPT), even when wind speeds are lower than anticipated.

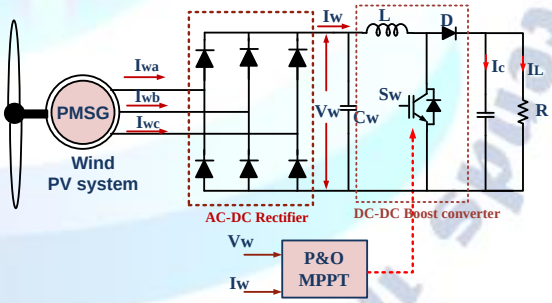

Figure .7 Typical diagram of wind-turbine system.

Reduced wind speeds lower the generator's power requirements. Many people are hopeful that maximum power point tracking (MPPT) may improve power plant efficiency [33]. The voltage is raised or lowered by adjusting the duty cycle of the power side converter. But MPPT may increase the generator's output. This experiment used a P&O algorithm; however there are other MPPT approaches available.

C. Perturb and Observe Algorithm

One possible use of the PO algorithm [27] is to find the machine's ideal configuration. According to this research, the best way for a PMSG generator to be installed in a wind turbine is such that it can produce the most electricity. Changing the DC voltage at the converter on the generator side is all that's required to control the power output. You will need a step-size (ΔD) and a time interval in order to monitor and manage these changes. The ratio of the current variable to the preceding variable (power output) is denoted by ΔD, while the percentage change in power is represented by ΔP. If the quantity of power generated increases, the value of the variable ΔD will stay the same, but if it drops, it will change. An enhanced PO approach, shown in Figure 8, uses a number of beginning factors to repeatedly change the step size. Another part of this strategy is figuring out how high of a duty cycle the boost converter can handle. One of the many benefits of developing this PO algorithm is the avoidance of oscillation problems caused by fluctuations in power at maximum value. The revised ΔD value in the improved approach is expected to reduce this, allowing the computation to converge faster. The basic structure of the original PO algorithm is preserved in this form, but the step size of each iteration is adjusted based on the system's response to the constant C. Determining the highest permissible duty cycle is also critical for the system to function within the constraints of the buck converter. At each run iteration, a time delay must be imposed so that the programme may respond to changes in the prescribed duty cycle.

Table 2. Parameters of permanent magnet synchronous generator (PMSG).

Description	Ratings
Stator phase resistance Rs (ohm)	0.0485Ω
Inductances [Ld(H) Lq(H)]	0.395e-3H
Rotor type	Salient type
Line Voltage constant (V)	150.6271V
Flux linkage	0.13841Wb
Torque constant N.m	1.2457
Inertia J(kg.m^2)	0.000027
viscous damping F(N.m.s)	4
pole pairs	6

D. DC-DC Boost Converter Units

A conventional DC-DC Boost converter is an efficient and practical way to connect the PV source and wind system to the common DC link capacitor. Its simple design, few converter components, and high conversion efficiency make it ideal for this task [34]. This converter can increase the low voltage from renewable sources to the desired value by changing the duty cycle at a higher switching frequency rate. As shown in Figure 9, every power supply has one semiconductor switch (S), one diode (D), one inductor (L), and one capacitor (C). The inductor L is essential for the boost converter to work. The input and output voltages are significantly different [35]. Equations (8), (9) and (10), when applied, provide the voltage transfer gain, current, and output voltage. Finding the Boost converter's transfer gain, output voltage, and output current is done using the equation found in [36].

$$V_o = \left(\frac{1}{1-D}\right) V_{PV} \quad (8)$$

$$I_0 = \left(\frac{1}{1-D}\right) V_{PV} \quad (9)$$

$$M = \frac{V_o}{V_{PV}} = \frac{1}{1-D} \quad (10)$$

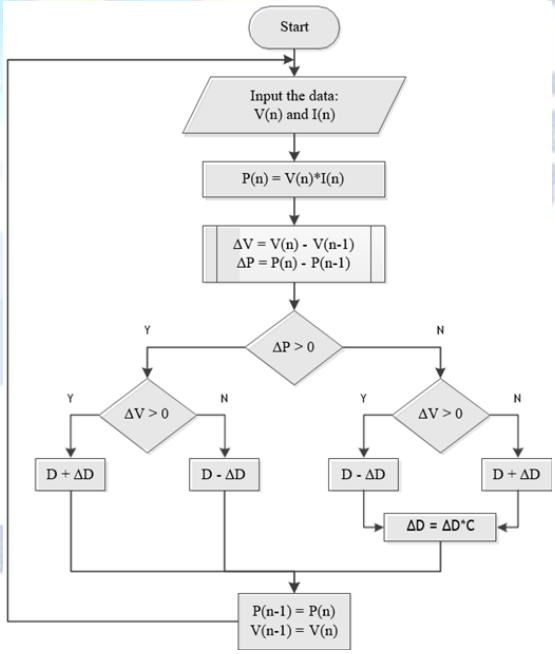

Figure .8 Flow chart of perturb and observe algorithm for wind DC-DC converter.

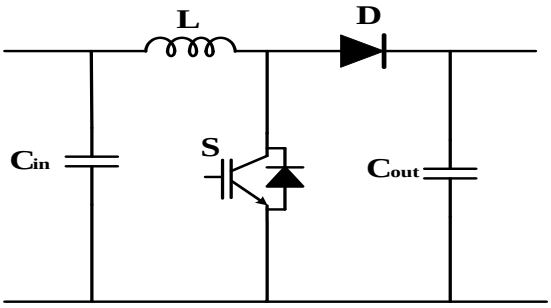

FIGURE 9. Equivalent circuit of conventional Boost converter

Vpv, Io, and Vo are the voltage, current, and output voltage of a PV system, respectively, shown here. There is a relationship between voltage transfer gain (M) and duty cycle (D). Boost converter simulation settings are included in Table 1, and Figure 10 depicts the theoretical switching waveform of the same.

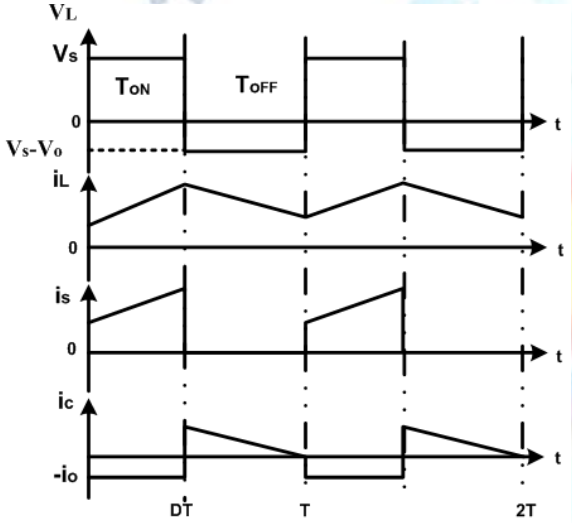

FIGURE 10. Switching waveform of Boost Converter

TABLE 3. Parameters of the boost converter

Description	Ratings
Input voltage, Vin	130V
Output voltage, Vout	200 V
Boost inductor, L	1.5e-3H
DC link capacitors, C	3300e-6 F
Load resistance, R	97.5Ω
Switching frequency, fs	10 kHz

E. BESS CONVERTER CONFIGURATION

In DC microgrid systems, voltage optimisation aims to maximise distribution efficiency while avoiding transformations. The DC system can easily accommodate a 48 V solar panel feeder. Figure 11 shows the bidirectional DC converter connecting the ESSs to the DC bus. It is common practice to install a DC-DC converter system between the DC bus and the energy storage device at the interface to reduce DC voltage variations. The responsiveness, dependability, and efficiency of the system depend on the bidirectional converter's capacity to function well in any operational mode.

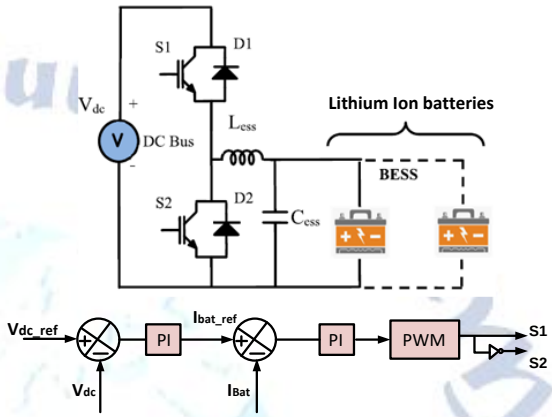

FIGURE 11. Battery Energy Management using a Bidirectional DC-DC Converter.

Mode 1: While the battery is charging, turn on switch S1 and diode D2 to put the converter into buck mode.

Mode 2: In order to meet the DC bus demand during power outages, switch S2 and diode D1 are turned on, and the converter is run in boost mode.

Mode 3: Charging batteries slowly (in float mode) while they're not in use keeps their voltage and charge level constant.

The open circuit voltage (OCV) was used to determine the battery's state of charge (SoC), as explained in Reference [37]. Alterations to the state of charge (SoC) of the battery are proportional to variations in operational current voltage (OCV). The connection between Lithium Ion Battery SoC and OCV is shown by this equation.

$$V_{oc}(t) = a_n XSoC(t) + a_0 \quad (11)$$

Take the terminal voltage at 0% SoC (a_o) as an example; it can be calculated using the open-circuit voltage at 100% SoC (a_n) of the battery.

F. ELECTRIC VEHICLE CONVERTER CONFIGURATION

An essential part of charging stations and other external power sources for electric vehicles (EVs) is the bidirectional converter. It enables dynamic regulation of energy flow according to the demands of the vehicle

and grid circumstances, allowing for flexible charging and discharging. Power can be efficiently transferred from the electric vehicle's battery to external power sources and back again thanks to the bidirectional DC-DC converter. The charging and discharging process is optimised using complex control algorithms, resulting in maximum energy efficiency and minimal power losses. By combining customer preferences with real-time data, a hybrid learning algorithm can adapt its operation to changing grid circumstances and charging needs. Overall grid stability and efficiency are both improved by this smart management technology, which also improves the operation of the EV charging infrastructure. When it comes to the integration of energy storage into the electric vehicle ecosystem, the bidirectional converter is crucial. It allows for the efficient transfer of excess energy from renewable sources or the grid to the battery of the EV. Additionally, it makes it easier to release energy that has been stored in the event of grid instability or heavy demand. Ultimately, the bidirectional DC-DC converter promotes sustainable transportation options by serving as an intelligent and adaptable interface within the electric vehicle charging infrastructure.

Mode 1: Battery Charging (Buck Mode)

- Switch S1 and Diode D2 Operation**:** In this state, the switch S1 is closed and the diode D2 is forward biassed. Diode D2 ensures that current can only flow in one way, while the electric vehicle's battery gets power from an external source (such a charging station) via the closed switch.
- Buck Mode Operation: Buck mode allows the converter to work with the lower voltage of the electric vehicle's battery by reducing the voltage from the external power source. Making ensuring the battery receives the correct voltage is crucial for efficient charging.
- Charging the Battery: Power is efficiently supplied to the electric vehicle's battery from an outside source. By adjusting the duty cycle of the switch, one may get the desired voltage conversion ratio when working in buck mode. For buck mode, these are the primary formulas:

Voltage Conversion Ratio (Duty Cycle, D): $D = \frac{V_{out}}{V_{in}}$

Inductor Current (I_L): $Vout = \frac{V_{in} \times (1-D)}{D \times (1-D) \times I_L}$

Output Power (Pout): $Pout = V_{out} \times I_L$

Efficiency (η): $\eta = \frac{P_{Out}}{P_{in}} \times 100\%$

Mode 2: Battery Discharging for Power Delivery (Boost Mode)

- **Switch S2 and Diode D1 Operation:** This mode is initiated by passing current via diode D1 and closing switch S2. By closing the switch, diode D1 ensures that current can only flow in one way, allowing the electric motor and other loads to receive power from the EV battery.
- **Boost Mode Operation:** When the converter is in boost mode, it charges the battery of the electric car to the voltage needed by the load. Crucial for maintaining power to the vehicle's systems in the event that the voltage applied to the load surpasses that of the battery.
- **Power Delivery:** The electric vehicle can drive and perform its functions by transferring energy from its battery to its load. Controlling the duty cycle of the switch allows one to achieve the desired voltage conversion ratio while working in boost mode. The following formulas are necessary to boost mode:

Voltage Conversion Ratio (Duty Cycle, D): $D = \frac{1}{1-\left(\frac{V_{out}}{V_{in}}\right)}$

Inductor Current (I_L): $Vout = \frac{V_{in}}{(1-D) \times I_L}$

Output Power (Pout): $Pout = V_{out} \times I_L$

Efficiency (η): $\eta = \frac{P_{Out}}{P_{in}} \times 100\%$

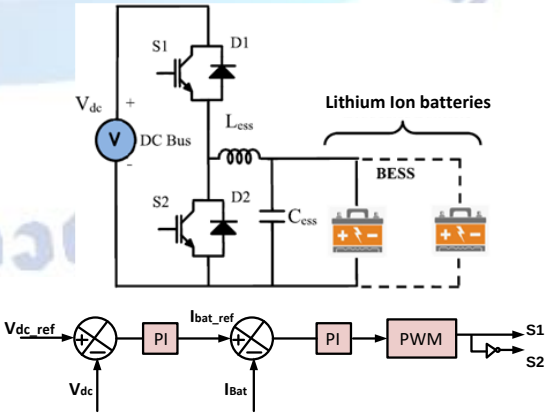

FIGURE 10. Bidirectional DC-DC converter configuration for Electric Vehicle Battery charging.

IV. RESULTS AND DISCUSSION

Three distinct experiments of a hybrid renewable energy microgrid were conducted in the study. In the first scenario, we evaluated the microgrid in an optimal environment with perfect weather that would allow all renewable energy sources to run at maximum efficiency. The second case study replicated real-world circumstances where changes in wind speed and renewable sun irradiation might affect the microgrid's output. The battery for renewable power production acted as a backup and provided electricity during periods of low generation, ensuring a consistent and reliable supply of energy. Furthermore, it enhanced microgrid stability by controlling the charging station's power use in reaction to unforeseen variations in demand. In the third scenario, the battery of the electric car was charged to speed up the charging process and ensure that it wouldn't be interrupted. The battery may be able to store excess energy from renewable sources during times of low demand and make it available for charging when needed. By doing this, the demand on non-renewable power sources is reduced and the amount of renewable energy used to power EVs is increased.

A. Constant State of Renewable Energy Sources at Maximum Capacity

In the first scenario, the objective is to have a steady stream of energy coming from a renewable source that powers and charges the battery of the electric car. By doing this, it meets the power needs of the electric vehicle and its battery while also maximising the usage of renewable energy sources. The electric car's battery can be charged by renewable energy sources, which might allow it to continue operating even if the primary power source fails. The argument also has the advantage of lowering carbon emissions and reliance on non-renewable energy sources. The electric vehicle's battery charges more rapidly and extends its range between charges when the sun is shining the brightest and the wind is blowing the fastest, as shown in Figure 12. This serves two purposes: it maximises the amount of energy harvested from renewable sources, which promotes sustainability, while also increasing overall system efficiency.

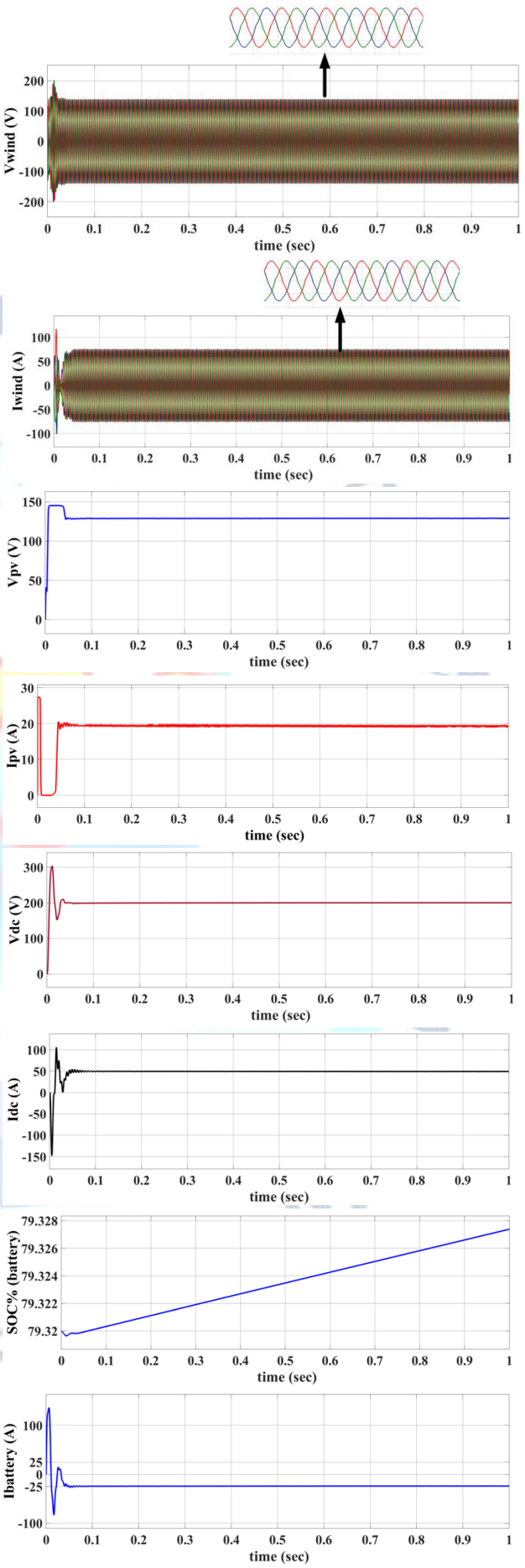

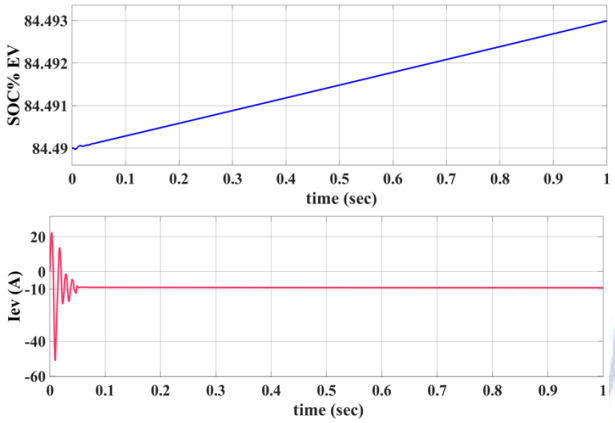

FIGURE 12. steady state condition operating renewable energy sources with maximum capacity

B. Dynamic performance of renewable energy generation in response to climate change

The efficiency and reliability of renewable energy sources will be impacted by climate change-related shifts in wind speeds and solar irradiation. From zero seconds to thirty-five seconds, the sun's irradiance will decrease from one thousand W/m^2 to zero W/m^2, as seen in Figure 13. The efficiency with which solar panels generate electricity is dependent on the amount of sunlight reaching those collectors. In the same time as the wind speed decreases with changes in wind direction, the wind speed will fall from 12 m/s to 0 m/s in around 0.75 to 1 second. Since renewable energy sources continually replenish the electric car's battery, the energy input is never-ending. We need a system that integrates renewable energy sources with battery storage to guarantee that electric vehicles and other electrical devices always have access to power. Also, when renewable energy production is strong, batteries make good use of the surplus. During periods of low output or high demand, this surplus energy may be stored and used. Fig. 13 displays the climate-related fluctuations in electric vehicle battery discharge and renewable energy supply. As seen in Figure 3, the energy storage device maintains a DC bus voltage of 200V to guarantee power balance.

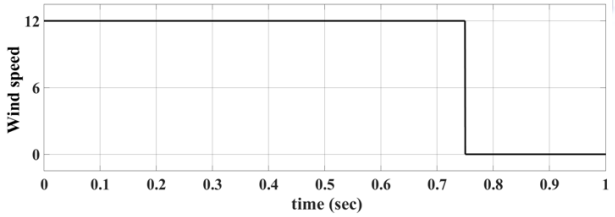

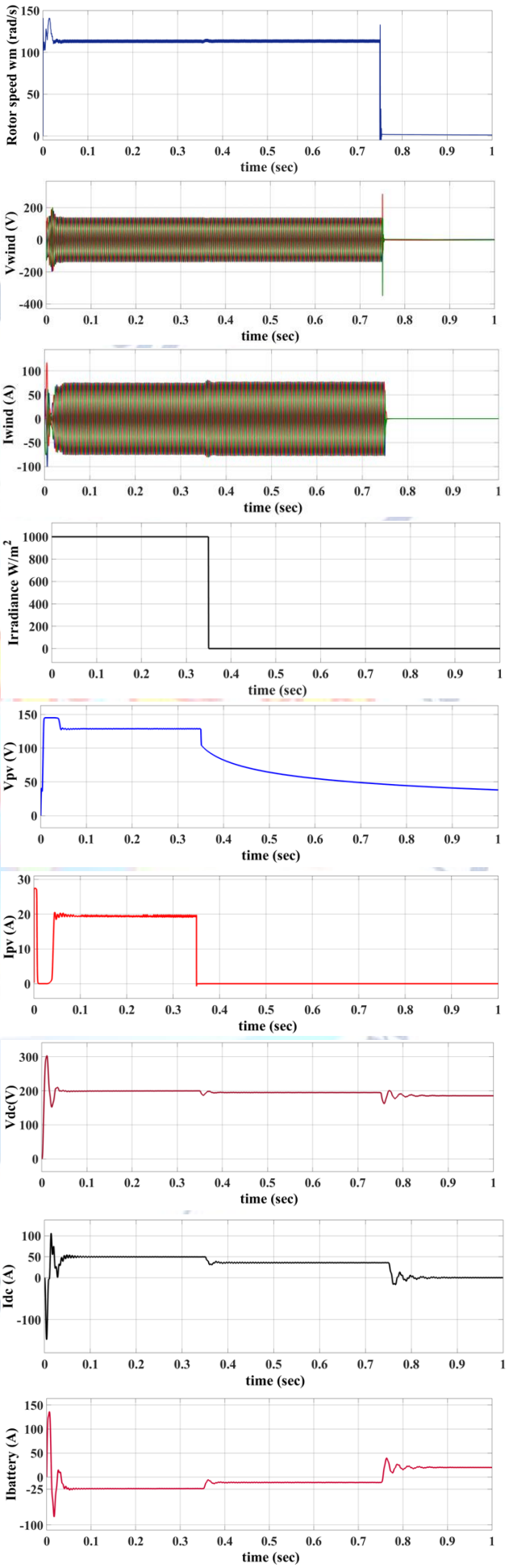

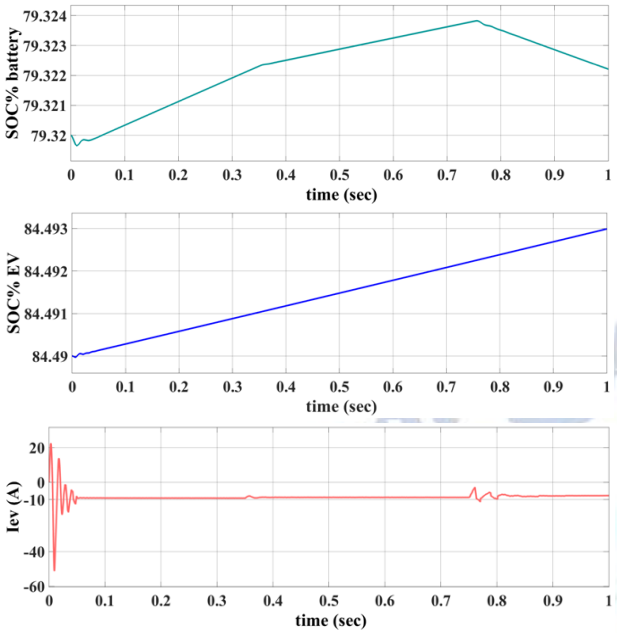

FIGURE 13. Dynamic condition of different operating mode of renewable energy sources

C. power fluctuation in various operating modes

Taking into account particular variations in solar irradiation and wind speed over time, the power fluctuations of the integrated charging system are carefully examined in the simulated scenario across different operating modes as shown in figure .14. Throughout the day, solar irradiation changes from 1000 W/m^2 to 0 W/m^2 over a certain time period, reflecting the ever-changing nature of sunshine exposure. Fluctuations in cloud cover, shading, and atmospheric conditions cause solar irradiance to shift dynamically within a precise timescale of 0 to 0.35 seconds, reflecting the complex fluctuations in sunlight exposure. These variations clearly demonstrate how solar energy is intermittent and how it affects the dynamics of electricity production. During a given time period, wind speed may range from 12 m/s to 0 m/s, depending on atmospheric conditions, geography, and weather patterns. Over a somewhat longer timescale, ranging from 0.75 to 1 second intervals, the system painstakingly records variations in wind speed. These variations do a good job of capturing the subtle variations in wind speed due to geographical features, atmospheric pressure gradients, and localized weather patterns. The dynamic nature of wind energy as a renewable power source is best shown by such thorough modeling. The simulation analyses the changing load power consumption of a charging station and linked devices over time, revealing the operational dynamics of the system. Power demand from various electric cars and their interactions with the grid are what cause these variations. The simulation time is also monitored for variations in EV power use, demonstrating the system's flexibility in real-world situations. The power profile of the battery shows dynamic charging and discharging cycles over time, connected to renewable energy storage and distribution for EV charging. These variations demonstrate the system's ability to handle different climatic conditions and operating needs. The simulation provides insights into the integrated charging system's temporal stability and flexibility, emphasizing the importance of advanced adaptive charging algorithms like the Maximum Power Point Tracking (MPPT) algorithm for optimal use of renewable energy and system reliability in changing environments.

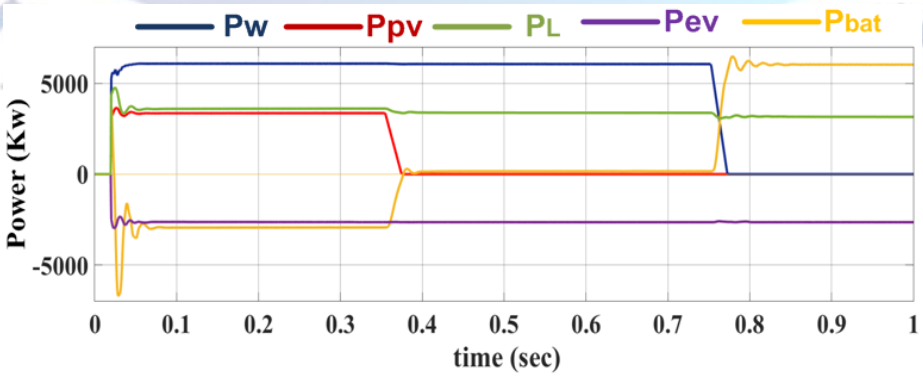

FIGURE 12. Simulation results of power fluctuation in various operating modes.

V. Conclusion

The integration of wind and solar technologies into electric vehicle (EV) charging infrastructure, combined with battery microgrids in a DC fast charging architecture, offers a promising solution for sustainable mobility. This approach reduces environmental impact and enhances energy resilience. The Perturb and Observe Maximum Power Point Tracking (MPPT) algorithm optimizes charging processes, ensuring efficient utilization of renewable energy sources. The system can adapt to changing environmental conditions and dynamically adjust charging parameters to maximize energy capture. Battery microgrids ensure uninterrupted EV charging, especially during climate change-induced disruptions. The surplus energy stored in station batteries acts as backup power and contributes to grid stability and reliability. This study highlights the importance of renewable energy integration and efficient charging algorithms in driving the transition towards environmentally friendly transportation solutions. Prioritizing widespread adoption of these technologies is crucial to realize the full potential of sustainable mobility initiatives and mitigate the adverse effects of climate change.

Conflict of interest statement

Authors declare that they do not have any conflict of interest

References

[1] H. T. Dinh, J. Yun, D. M. Kim, K. Lee, and D. Kim, ``A home energy management system with renewable energy and energy storage utilizing main grid and electricity selling,'' IEEE Access, vol. 8, pp. 49436_49450, 2020.

[2] C. Byers and A. Botterud, ``Additional capacity value from synergy of variable renewable energy and energy storage,'' IEEE Trans. Sustain. Energy, vol. 11, no. 2, pp. 1106_1109, Apr. 2020.

[3] M. Rizwan, L. Hong, W. Muhammad, S. W. Azeem, and Y. Li, ``Hybrid Harris Hawks optimizer for integration of renewable energy sources considering stochastic behavior of energy sources,'' Int. Trans. Elect. Energy Syst., vol. 31, no. 2, 2021, Art. no. e12694, doi: 10.1002/2050- 7038.12694.

[4] Y. Sun, Z. Zhao, M. Yang, D. Jia,W. Pei, and B. Xu, ``Overview of energy storage in renewable energy power fluctuation mitigation,'' CSEE J. Power Energy Syst., vol. 6, no. 1, pp. 160_173, 2020.

[5] T. Salameh, M. A. Abdelkareem, A. G. Olabi, E. T. Sayed, M. Al-Chaderchi, and H. Rezk, ``Integrated standalone hybrid solar PV, fuel cell and diesel generator power system for battery or supercapacitor storage systems in khorfakkan, united arab emirates,'' Int. J. Hydrogen Energy, vol. 46, no. 8, pp. 6014_6027, Jan. 2021.

[6] M. Çolak and Ä. Kaya, ``Multi-criteria evaluation of energy storage technologies based on hesitant fuzzy information: A case study for turkey,'' J. Energy Storage, vol. 28, Apr. 2020, Art. no. 101211.

[7] M. A. Hannan, M. M. Hoque, A. Mohamed, and A. Ayob, ``Review of energy storage systems for electric vehicle applications: Issues and challenges,'' Renew. Sustain. Energy Rev., vol. 69, pp. 771_789, Mar. 2017.

[8] R. Amirante, E. Cassone, E. Distaso, and P. Tamburrano, ``Overview on recent developments in energy storage: Mechanical, electrochemical and hydrogen technologies,'' Energy Convers. Manage., vol. 132, pp. 372_387, Jan. 2017.

[9] T. Ma, H.Yang, and L. Lu, ``Development of hybrid battery supercapacitor energy storage for remote area renewable energy systems,'' Appl. Energy, vol. 153, pp. 56_62, Sep. 2015.

[10] X. Wang, D. Yu, S. Le Blond, Z. Zhao, and P. Wilson, ``A novel controller of a battery-supercapacitor hybrid energy storage system for domestic applications,'' Energy Buildings, vol. 141, pp. 167_174, Apr. 2017.

[11] A. Kadri, H. Marzougui, A. Aouiti, and F. Bacha, ``Energy management and control strategy for a DFIG wind turbine/fuel cell hybrid system with super capacitor storage system,'' Energy, vol. 192, Feb. 2020, Art. no. 116518.

[12] A. K. Barik, D. C. Das, A. Latif, S. M. S. Hussain, and T. S. Ustun, ``Optimal voltage_frequency regulation in distributed sustainable energybased hybrid microgrids with integrated resource planning,'' Energies, vol. 14, no. 10, p. 2735, May 2021, doi: 10.3390/en14102735.

[13] A. K. Barik, S. Jaiswal, and D. C. Das, ``Recent trends and development in hybrid microgrid: A review on energy resource planning and control,'' Int. J. Sustain. Energy, vol. 4, pp. 1_15, Apr. 2021, doi: 10.1080/14786451.2021.1910698.

[14] H. Kakigano, Y. Miura, and T. Ise, ``Distribution voltage control for DC microgrids using fuzzy control and gain-scheduling technique,'' IEEE Trans. Power Electron., vol. 28, no. 5, pp. 2246_2258, May 2013.

[15] D. A. Aviles, J. Pascual, F. Guinjoan, G. G. Gutierrez, R. G. Orguera, J. L. Proano, P. Sanchis, and T. E. Motoasca, ``An energy management system design using fuzzy logic control: Smoothing the grid power profile of a residential electro-thermal microgrid,'' IEEE Access, vol. 9, pp. 25172_25188, 2021.

[16] M. Kumar, S. C. Srivastava, and S. N. Singh, ``Control strategies of a DC microgrid for grid connected and islanded operations,'' IEEE Trans. Smart Grid, vol. 6, no. 4, pp. 1588_1601, Jul. 2015.

[17] H. Hajebrahimim, S. M. Kaviri, S. Eren, and A. Bakhshai, ``A new energy management control method for energy storage systems in microgrids,'' IEEE Trans. Power Electron., vol. 35, no. 11, pp. 11612_11624, Mar. 2020.

[18] Y. Xu and X. Shen, ``Optimal control based energy management of multiple energy storage systems in a microgrid,'' IEEE Access, vol. 6, pp. 32925_32934, 2018.

[19] A.-R.-I. Mohamed, H. H. Zeineldin, M. M. A. Salama, and R. Seethapathy,``Seamless formation and robust control of distributed generation microgrids via direct voltage control and

optimized dynamic power sharing," IEEE Trans. Power Electron., vol. 27, no. 3, pp. 1283_1294, Mar. 2012.

[20] B. A. Martinez-Treviño, A. El Aroudi, E. Vidal-Idiarte, A. Cid-Pastor, and L. Martinez-Salamero, ``Sliding-mode control of a boost converter under constant power loading conditions," IET Power Electron., vol. 12, no. 3, pp. 521_529, 2019.

[21] T. K. Roy, M. A. Mahmud, A. M. T. Oo, M. E. Haque, K. M. Muttaqi, and N. Mendis, ``Nonlinear adaptive backstepping controller design for islanded DC microgrids," IEEE Trans. Ind. Appl., vol. 54, no. 3, pp. 2857_2873, May 2018.

[22] A. Iovine, M. J. Carrizosa, G. Damm, and P. Alou, ``Nonlinear control for DC microgrids enabling ef_cient renewable power integration and ancillary services for AC grids," IEEE Trans. Power Syst., vol. 34, no. 6, pp. 5136_5146, Nov. 2019.

[23] X. Li, X. Zhang,W. Jiang, J.Wang, P.Wang, and X.Wu, ``A novel assorted nonlinear stabilizer for DC_DC multilevel boost converter with constant power load inDCmicrogrid," IEEE Trans. Power Electron., vol. 35, no. 10, pp. 11181_11192, Oct. 2020.

[24] J. Wu and Y. Lu, ``Adaptive backstepping sliding mode control for boost converter with constant power load," IEEE Access, vol. 7, pp. 50797_50807, 2019.

[25] M. G. Villalva, J. R. Gazoli, and E. R. Filho, "Comprehensive approach to modeling and simulation of photovoltaic arrays," IEEE Transactions on Power Electronics, vol. 24, no. 5, pp. 1198–1208, 2009.

[26] Syahputra, R.; Wiyagi, R.O.; Sudarisman. Performance Analysis of a Wind Turbine with Permanent Magnet Synchronous Generator. J. Theor. Appl. Inf. Technol. 2017, 95, 1950–1957.

[27] Farhat, S.; Alaoui, R.; Kahaji, A.; Bouhouch, L.; Ihlal, A. P&O and Incremental Conductance MPPT Implementation. Int. Rev. Electr. Eng. 2015, 10, 116–122.

[28] Al Hasibi, R.A.; Hadi, S.P.; Sarjiya, S. Integrated and Simultaneous Model of Power Expansion Planning with Distributed Generation. Int. Rev. Electr. Eng. 2018, 13, 116–127.

[29] Metry, M.; Shadmand, M.B.; Balog, R.S.; Abu-Rub, H. MPPT of Photovoltaic Systems Using Sensorless Current-Based Model Predictive Control. IEEE Trans. Ind. Appl. 2017, 53, 1157–1167.

[30] Soetedjo, A.; Lomi, A.; Mulayanto, W.P. Modeling of wind energy system with MPPT control. In Proceedings of the 2011 International Conference on Electrical Engineering and Informatics, Bandung, Indonesia, 17–19 July 2011; pp. 1–6.

[31] Zhang, Y.; Zhang, L.; Liu, Y. Implementation of Maximum Power Point Tracking Based on Variable Speed Forecasting for Wind Energy Systems. Processes 2019, 7, 158.

[32] Costanzo, L.; Schiavo, A.L.; Vitelli, M. Design Guidelines for the Perturb and Observe Technique for Electromagnetic Vibration Energy Harvesters Feeding Bridge Rectifiers. IEEE Trans. Ind. Appl. 2019, 55, 5089–5098.

[33] Raj, T.G.; Kumar, B.R. Comparative Analysis of Incremental Conductance and Perturb & Observe Mppt Methods For Single-Switch Dc/Dc Converter. In Proceedings of the 2018 National Power Engineering Conference (NPEC), Madurai, India, 9–10 March 2018.

[34] Kirubakaran A, Jain S, Nema RK. —The PEM fuel cell system with DC/DC boost converter: design, modeling and simulation‖. Int. J recent trends in Engineering, vol. 1, no. 3, pp. 157-161, 2009.

[35] Nejabatkhah F, Danyali S, Hosseini SH, Sabahi M, Niapour SM. —Modeling and control of a new three-input DC–DC boost converter for hybrid PV/FC/battery power system‖. IEEE Trans.PowerElectron., vol. 27, no. 5, pp. 2309-24, 2012.

[36] Revathi, B. Sri, and M. Prabhakar. "Non isolated high gain DC-DC converter topologies for PV applications–A comprehensive review." Renew. Sustain. Energy Rev., vol. 66, pp. 920-933, 2016.

[37] W.-Y. Chang, ``The state of charge estimating methods for battery: A review," ISRN Appl. Math., vol. 2013, pp. 1_7, Dec. 2013, doi: 10.1155/2013/953792.